Mechanism of the Enantioselective Dihydroxylation of Olefins by OsO_4 in the Presence of Chiral Bases[1]

Achim Veldkamp and Gernot Frenking*

Contribution from the Fachbereich Chemie, Philipps-Universität Marburg, D-35032 Marburg, Germany

Received September 24, 1993. Revised Manuscript Received March 4, 1994[⊗]

Abstract: Quantum mechanical ab initio calculations with complete geometry optimization using relativistic effective core potentials for osmium are reported for the postulated intermediates of the base-catalyzed addition reaction of OsO_4 (**1**) with olefins, using NH_3 and ethylene as model compounds. The energy of the HOMO of **1** is substantially raised upon complexation with NH_3. The four-membered cyclic species **3** suggested by Sharpless as an intermediate for the addition reaction is predicted to be a minimum on the potential energy hypersurface. Structure **3** is calculated to be 30.5 kcal mol^{-1} (QCISD(T) + ZPE) higher in energy than the five-membered cyclic isomer **2**. Both isomers are strongly stabilized by complexation with ammonia. The Os–NH_3 binding energy is significantly higher in **2(NH_3)** and **3(NH_3)** than in **1(NH_3)**, which explains the acceleration of the addition reaction in the presence of a base. The formation of **2(NH_3)** from **1(NH_3)** and ethylene is exothermic, while the formation of **3(NH_3)** is calculated to be slightly endothermic by about 5–10 kcal mol^{-1}. The energy calculations suggest that **3(NH_3)** is initially formed in a [2 + 2] concerted reaction with a nucleophilic and an electrophilic phase, followed by isomerization to **2(NH_3)**. The complexes **1(2NH_3)** and **2(2NH_3)**, which have two ammonia ligands, are also calculated as energy minimum structures. The asymmetric five-membered cyclic isomer **2a(2NH_3)**, with one axial and one equatorial ammonia group, which is suggested by Corey as the initial reaction product, is another minimum on the potential energy surface. Structure **2a(2NH_3)** is predicted to be 24.2 kcal mol^{-1} less stable than the isomer **2(2NH_3)**. The calculations also indicate the formation of dimeric structures as possible intermediates. Complex **1(NH_3)** may form the dimer **5(2NH_3)** with four idential Os–O bonds. The addition of two molecules of ethylene to **5(2NH_3)** yields the complex **4(2NH_3)**. The geometry-optimized intermediates of the second reaction cycle with low enantioselectivity postulated by Sharpless are discussed. The comparison of the theoretically predicted geometries with the experimental structures show good agreement.

1. Introduction

It has been known for some time that the old[2] and well-established[3] oxidation of alkenes with osmium tetraoxide to form cis diols is accelerated in the presence of ammines[4] and that chiral bases may induce an asymmetric osmylation of the olefins.[5–7] This reaction has been intensively investigated in the last years by several groups,[5–10] in particular since Sharpless developed a catalytic version[5c] of the asymmetric dihydroxylation which employs cinchona alkaloids. In spite of considerable experimental efforts,[5–10] however, the mechanism of the reaction is still unclear, and several questions have not been answered yet. Should the reaction be considered as an electrophilic or as a nucleophilic attack on the olefin by osmium tetraoxide? If the osmium atom is directly involved in the primary attack, then OsO_4 should react as an electrophile because of the highly electron-deficient Os(VIII) atom. If only the oxygen atoms are involved, then the reaction would be a nucleophilic attack. Then, what causes the acceleration of the reaction in the presence of a base? Of particular interest is the question of how chirality is transmitted from the chiral alkaloid ligand to the Os(VI) ester complex formed during the reaction. Because the chiral bases are usually very bulky,[10] it might be assumed that the asymmetric induction is caused by steric interactions. But it has recently been demonstrated[8] that stereoelectronic control plays an important role in the osmium tetraoxide-induced dihydroxylation of alkenes when steric factors are removed.

Several explanations have been offered to rationalize the observed enantioselectivity. Sharpless suggested[5b,c] that the initial

---

[⊗] Abstract published in *Advance ACS Abstracts,* May 1, 1994.

[1] Theoretical Studies of Organometallic Compounds. 8. For part 7, see: Ehlers, A. W.; Frenking, G. *J. Am. Chem. Soc.* **1994**, *116*, 1514.

[2] Makowka, O. *Ber. Dtsch. Chem. Ges.* **1908**, *41*, 943.

[3] See, e.g.: (a) March, J. *Advanced Organic Chemistry*; McGraw-Hill: New York, 1985; p 732. (b) Vollhardt, K. P. C. *Organic Chemistry*; VCH Publishers: Weinheim, 1988; p 492. (c) Schröder, M. *Chem. Rev.* **1980**, *80*, 187.

[4] Criegee, R.; Marchand, B.; Wannowius, H. *Liebigs Ann. Chem.* **1942**, *550*, 99.

[5] (a) Sharpless, K. B.; Teranishi, A. Y.; Bäckvall, J.-E. *J. Am. Chem. Soc.* **1977**, *99*, 3120. (b) Hentges, S. G.; Sharpless, K. B. *J. Am. Chem. Soc.* **1980**, *102*, 4263. (c) Jacobsen, E. N.; Markó, I.; Mungall, W. S.; Schröder, G.; Sharpless, K. B. *J. Am. Chem. Soc.* **1988**, *110*, 1968. (d) Lohray, B. B.; Kalantar, T. H.; Kim, B. M.; Park, C. Y.; Shibata, T.; Wai, J. S. M.; Sharpless, K. B. *Tetrahedron Lett.* **1989**, *30*, 2041. (e) Svendson, J. S.; Markó, I.; Jacobsen, E. N.; Rao, C. P.; Bott, S.; Sharpless, K. B. *J. Org. Chem.* **1989**, *54*, 2263. (f) Wai, J. S. M.; Markó, I.; Svendsen, J. S.; Finn, M. G.; Jacobsen, E. N.; Sharpless, K. B. *J. Am. Chem. Soc.* **1989**, *111*, 1123. (g) Jacobsen, E. N.; Markó, I.; France, M. B.; Svendsen, J. S.; Sharpless, K. B. *J. Am. Chem. Soc.* **1989**, *111*, 737. (h) Kwong, H.-L.; Sorato, C.; Ogino, Y.; Chen, H.; Sharpless, K. B. *Tetrahedron Lett.* **1990**, *31*, 2999. (i) Shibata, T.; Gilheany, D. G.; Blackburn, B. K.; Sharpless, K. B. *Tetrahedron Lett.* **1990**, *31*, 3817. (j) Ogino, Y.; Chen, H.; Kwong, H.-L.; Sharpless, K. B. *Tetrahedron Lett.* **1991**, *32*, 3965. (k) Sharpless, K. B.; Amberg, W.; Beller, M.; Chen, H.; Hartung, J.; Kawanami, Y.; Lübben, D.; Manoury, E.; Ogino, Y.; Shibata, T.; Ukita, T. *J. Org. Chem.* **1991**, *56*, 4585. (l) Ogino, Y.; Chen, F.; Manoury, E.; Shibata, T.; Beller, M.; Lübben, D.; Sharpless, K. B. *Tetrahedron Lett.* **1991**, *32*, 5761. (m) Sharpless, K. B.; Amberg, W.; Bennani, Y. L.; Crispino, G. A.; Hartung, J.; Jeong, K.-S.; Kwong, H.-L.; Morikawa, K.; Wang, Z.-M.; Xu, D.; Zhang, X.-L. *J. Org. Chem.* **1992**, *57*, 2768. (n) Wang, L.; Sharpless, K. B. *J. Am. Chem. Soc.* **1992**, *114*, 7568. (o) Pearlstein, R. M.; Blackburn, B. K.; Davis, W. M.; Sharpless, K. B. *Angew. Chem.* **1990**, *102*, 710; *Angew. Chem., Int. Ed. Engl.* **1990**, *29*, 639. (p) Göbel, T.; Sharpless, K. B. *Angew. Chem.* **1993**, *105*, 1417. (q) Kolb, H. C.; Andersson, P. G.; Bennani, Y. L.; Crispino, G. A.; Jeong, K.-S.; Kwong, H.-L.; Sharpless, K. B. *J. Am. Chem. Soc.*, submitted.

[6] (a) Tomioka, K.; Nakajima, M.; Iitaka, Y.; Koga, K. *Tetrahedron Lett.* **1988**, *29*, 573. (b) Tomioka, K.; Nakajima, M.; Koga, K. *J. Chem. Soc., Chem. Commun.* **1989**, 1921. (c) Tomioka, K.; Nakajima, M.; Koga, K. *Tetrahedron Lett.* **1990**, *31*, 1741. (d) Tomioka, K.; Nakajima, M.; Koga, K. *J. Am. Chem. Soc.* **1987**, *109*, 6213.

[7] (a) Corey, E. J.; Jardine, P. D.; Virgil, S.; Yuen, P.-W.; Connell, R. D. *J. Am. Chem. Soc.* **1989**, *111*, 9243. (b) Corey, E. J.; Lotto, G. I. *Tetrahedron Lett.* **1990**, *31*, 2665. (c) Corey, E. J.; Noe, M. C.; Sarshar, S. *J. Am. Chem. Soc.* **1993**, *115*, 3828.

[8] Halterman, R. L.; McEvoy, M. A. *J. Am. Chem. Soc.* **1992**, *114*, 980.

[9] Hermann, W. A.; Eder, S. J.; Scherer, W. *Angew. Chem.* **1992**, *104*, 1371; *Angew. Chem., Int. Ed. Engl.* **1992**, *31*, 1345.

[10] For a recent review, see: Waldmann, H. *Nachr. Chem. Tech. Lab.* **1992**, *40*, 702.

0002-7863/94/1516-4937$04.50/0

Scheme 1. Reaction Course Including the Intermediate **3(L)** Suggested by Sharpless[5b,c]

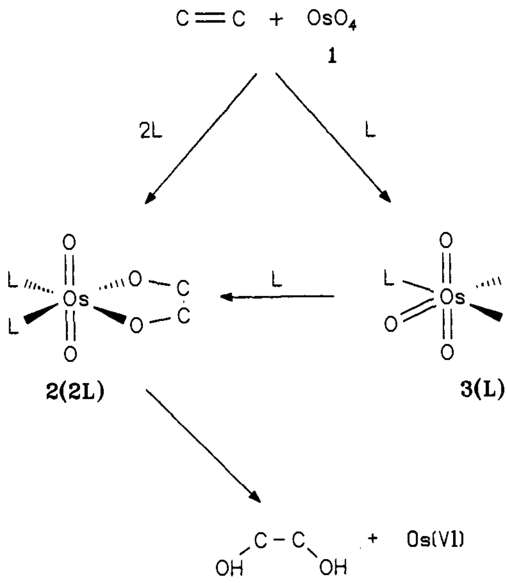

attack of OsO_4 (**1**) should proceed in the presence of a base ligand L via a coordination of the olefinic π bond to the metal center, forming the metallacycle intermediate **3(L)** (Scheme 1). In **3(L)**, the ligand L is in close proximity to the olefin, and the formation of the complex from **1(L)** and the olefin may therefore influence the stereoselectivity of the addition reaction. The four-membered cyclic structure **3(L)** should rearrange and then add a further base ligand L, forming the five-membered cyclic compound **2(2L)**, which is usually thought of as the addition product of a [3 + 2] cycloaddition reaction.[3] This stepwise mechanism was also suggested by Tomioka et al.[6a,c] to explain the observed stereochemical control. Hermann et al.[9] recently reported that fluorinated olefins can be oxidized catalytically by OsO_4, which indicates that the first reaction step must not be a nucleophilic attack of the olefin on the osmium. Jørgensen and Hoffmann[11] presented a theoretical analysis of the reaction using orbital symmetry arguments based on EHT calculations. These authors came to the conclusion that the [3 + 2] cycloaddition is symmetry allowed and that the reaction might proceed along this pathway, but the asymmetric intermediate **3** could not be ruled out.[11]

A different mechanism was postulated by Corey,[7] who proposed that the [3 + 2] cycloaddition may lead to an asymmetric octahedral intermediate **2a(2L)** in the presence of a bidentate base (Scheme 2).[7a] In the postulated precursor structure **1a(2L)**, the oxygen atoms in the five-membered ring are not equivalent, and the oxygen atom trans to the ligand group should be more nucleophilic than the other two oxygen atoms. The combined effects of electronic and steric interactions should then lead to the formation of **2a(2L)** in a [3 + 2] cycloaddition. A dimer OsO_4–base complex **5(2L)**, with electronically different oxygen atoms for reactions involving monodentate bases, was also suggested by Corey.[7b] The addition of **5(2L)** to olefins should yield **4(2L)** as product. The dimeric structure **4(2L)** has been observed in the solid.[12] In solution, however, **4(2L)** forms a monomeric complex.[12] This mechanism derived some support from kinetic studies reported by Corey et al.[7c] However, all kinetic measurements of the rate law for the addition reactions by Sharpless and co-workers[5g,q] and others[13,14] indicated *first-order* kinetics in OsO_4. This refutes the proposal of Corey et al.,[7] which

Scheme 2. Possible Reaction Pathway Suggested by Corey[7]

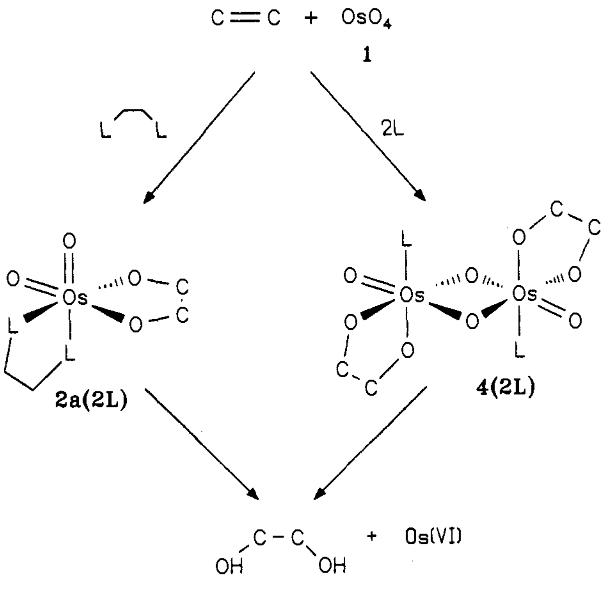

requires the rate law to be second-order in OsO_4. Also, the measured influence of the reaction temperature upon the enantioselectivity of the asymmetric dihydroxylation indicates a *two-step* mechanism for the addition reaction, which is inconsistent with a concerted [3 + 2] cycloaddition.[5p] Rather, a stepwise reaction with initial [2 + 2] addition was proposed.[5p] It should be pointed out that the kinetic measurements also indicate that *both* steps of the two-step mechanism exhibit stereoselectivity.[5p]

The reaction mechanism seems to have additional complexity: a detailed investigation of the reaction conditions for the catalytic dihydroxylation of olefins by OsO_4 in the presence of chiral bases prompted Sharpless to suggest[5f] that two reaction cycles are competing, one with high enantioselectivity and one with low enantioselectivity (Scheme 3). Structure **6** was proposed as a central intermediate for the two cycles, along with **7** and **8** as intermediates for the second cycle. This second cycle could later be shown to be suppressed when the osmylation was carried out in an aqueous/organic two-phase reaction employing $K_3[Fe(CN)_6]$ as the oxidant.[5j]

However, despite the information acquired about the mechanism, an explanation for the enantioselectivities observed could not be given. An X-ray analysis of an osmium tetraoxide–cinchona alkaloid complex demonstrated[5e] that the chiral center in the alkaloid ligand is quite remote from the oxo ligands. Therefore, it is unlikely that **1(L)** is responsible for the high enantioselectivity observed in the addition to alkenes.[5]

In order to give additional information on the possible reaction mechanism, we carried out quantum mechanical ab initio calculations using relativistic effective core potentials (ECP)[15] for osmium and all-electron basis sets for the other atoms.[16] In previous theoretical studies of transition-metal complexes[17] and osmium compounds,[18] we could show that the optimized geometries were in good agreement with experimental results if valence shell contraction schemes for the ECP[15] valence basis sets were employed which have been suggested in systematic studies of organometallic compounds.[19] In particular, the geometries of transition-metal compounds in *high* oxidation states predicted at

---

[11] Jørgensen, K. A.; Hoffmann, R. *J. Am. Chem. Soc.* **1986**, *108*, 1867.

[12] Cartwright, B. A.; Griffith, W. P.; Schröder, M.; Skapski, A. C. *J. Chem. Soc., Chem. Commun.* **1978**, 853.

[13] Burton, K. *Biochem. J.* **1967**, *104*, 686.

[14] Clark, R. L.; Behrman, E. J. *Inorg. Chem.* **1975**, *14*, 1425.

[15] Hay, P. J.; Wadt, W. R. *J. Chem. Phys.* **1985**, *82*, 299.

[16] (a) Binkley, J. S.; Pople, J. A.; Hehre, W. J. *J. Am. Chem. Soc.* **1980**, *102*, 939. (b) Hehre, W. J.; Ditchfield, R.; Pople, J. A. *J. Chem. Phys.* **1972**, *56*, 2257.

[17] (a) Jonas, V.; Frenking, G.; Reetz, M. T. *Organometallics* **1993**, *12*, 2111. (b) Veldkamp, A.; Frenking, G. *Organometallics* **1993**, *12*, 4613. (c) Stegmann, R.; Neuhaus, A.; Frenking, G. *J. Am. Chem. Soc.* **1993**, *115*, 11930. (d) Ehlers, A. W.; Frenking, G. *J. Chem. Soc., Chem. Commun.* **1993**, 1709. (e) Neuhaus, A.; Veldkamp, A.; Frenking, G. *Inorg. Chem.*, submitted.

[18] Veldkamp, A.; Frenking, G. *Chem. Ber.* **1993**, *126*, 1325.

Scheme 3. Mechanism of the Catalytic Two-Cycle Osmylation Suggested by Sharpless[5f]

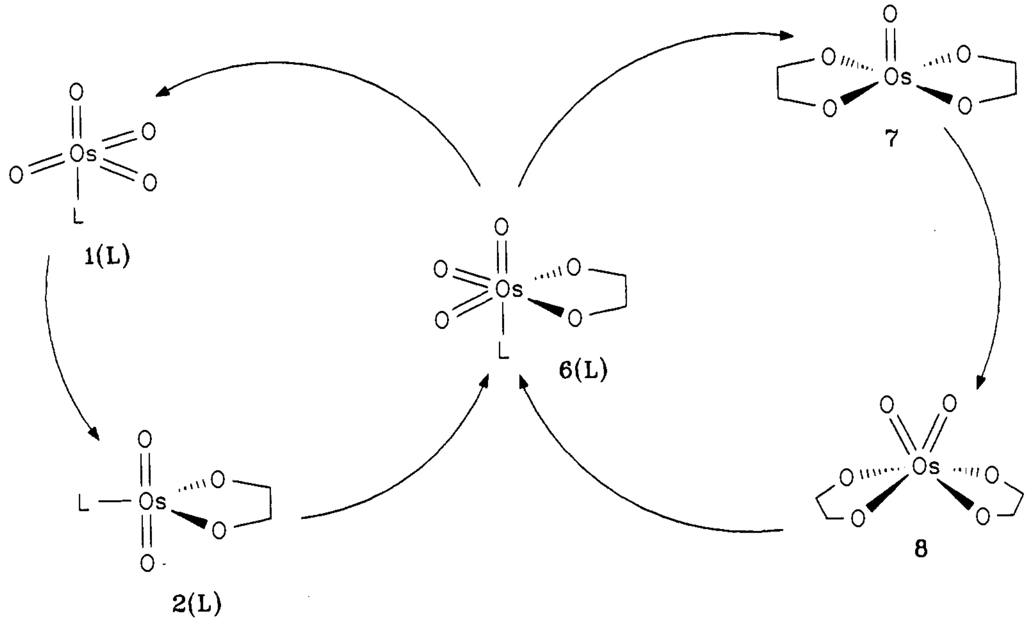

the Hartree–Fock level of theory are very similar to experimental values.[17a,c,e,18] We have calculated the geometries and relative energies of the structures **1**–**8**, which have been proposed as possible intermediates. In particular, the role of the ligand upon the reaction pathway was investigated, for which ammonia was chosen as a model.

2. Theoretical Details

All calculations were carried out using the program package Gaussian 92.[20] The geometries were optimized at the Hartree–Fock (HF) level of theory using a quasirelativistic effective core potential (ECP)[15] for osmium with a (441/41/21) basis set for the 16 "valence" electrons in conjunction with a 3-21G basis set for all other atoms.[16a] This basis set is denoted BS I. The vibrational frequencies and zero-point vibrational energies (ZPE) were calculated for all structures except **4(2NH$_3$)** and **4a(2NH$_3$)** using numerical second derivatives. All structures for which vibrational frequencies were calculated have positive eigenvalues of the Hessian matrix. Improved total energies were computed at the QCISD(T) level[21] using the same ECP[15] with a (441/2111/21/1) valence basis set for Os, which is augmented by a set of f-type polarization functions (exponent 0.886),[22] and a 6-31G(d) basis set for the other atoms.[16b] A set of five primitives was employed for the d-type polarization functions. This basis set is denoted BS II. Correlation energy was also calculated using Møller–Plesset perturbation theory terminated at second (MP2) and third (MP3) order.[23] Unless otherwise noted, energy differences discussed in this paper are given at QCISD(T)/II + ZPE or MP3/II + ZPE at geometries optimized at HF/I.[24] The ZPE values are scaled by 0.9.

3. Results and Discussion

The calculated total energies are shown in Table 1. Table 2 shows the theoretically predicted reaction energies for complex formation reactions. For some reactions (for example, reactions 3 and 5), the predicted reaction energies at MP2 and MP3 are very different. Oscillating energies calculated at different orders of Møller–Plesset perturbation theory for transition-metal compounds have been noted before.[25] The QCISD(T) results are more reliable and should be used in these cases.[24] Figure 1 shows the optimized structures and the most important bond lengths and angles calculated at HF/I.

We begin the discussion by examining the results for OsO_4 (**1**) and its base adducts **1(NH$_3$)** and **1(2NH$_3$)**. The geometry of **1** is predicted to have an Os–O distance of 1.686 Å, shorter than the experimentally reported[26] value of 1.711 Å. Complexation of OsO_4 by ammonia yields slightly longer Os–O bonds cis to NH_3 (1.701 Å), whereas the trans Os–O bond length in **1(NH$_3$)** is the same as that in **1** (Figure 1). The Os–N interatomic distance calculated for **1(NH$_3$)** (2.369 Å) agrees very well with the experimentally determined[27] Os–N bond length for the OsO_4–quinuclidine complex (2.37 Å). For the OsO_4–cinchona alkaloid complex, an Os–N distance of 2.49 Å has been measured.[5e] This shows that the OsO_4–ammine bond length is calculated with reasonable accuracy at this level of theory.[28] The binding energy between OsO_4 and NH_3 in **1(NH$_3$)** calculated at MP2/II + ZPE is 10.5 kcal mol^{-1}. At MP3/II + ZPE, the theoretically predicted OsO_4–NH_3 bond energy is slightly lower (7.8 kcal mol^{-1}, Table 2). There are no experimental values known to us for the binding energies of OsO_4 complexes.

A very interesting result calculated for **1(NH$_3$)** is the dramatic increase in the energy level of the highest occupied molecular

---

(19) Jonas, V.; Frenking, G.; Reetz, M. T. *J. Comput. Chem.* **1992**, *13*, 919.

(20) Frisch, M. J.; Trucks, G. W.; Head-Gordon, M.; Gill, P. M. W.; Wong, M. W.; Foresman, J. B.; Schlegel, H. B.; Raghavachari, K.; Robb, M. A.; Binkley, J. S.; Gonzalez, C.; Martin, R.; Fox, D. J.; Defrees, D. J.; Baker, I.; Stewart, J. J. P.; Pople, J. A. *Gaussian 92*, Revision A; Gaussian Inc.: Pittsburgh, PA, 1992.

(21) Pople, J. A.; Head-Gordon, M.; Raghavachari, K. *J. Chem. Phys.* **1987**, *87*, 5968.

(22) Ehlers, A. W.; Böhme, M.; Dapprich, S.; Gobbi, A.; Höllwarth, A.; Jonas, V.; Köhler, K. F.; Stegmann, R.; Veldkamp, A.; Frenking, G. *Chem. Phys. Lett.* **1993**, *208*, 111.

(23) (a) Møller, C.; Plesset, M. S. *Phys. Rev.* **1934**, *46*, 618. (b) Binkley, J. S.; Pople, J. A. *Int. J. Quantum Chem.* **1975**, *9S*, 229.

(24) The relative energies of structures such as **2** and **3** can be reliably calculated at the QCISD(T) level but not at MPn, because the coordination around the metal atom is different. The relative energies for **2** and **3** obtained at different orders of perturbation theory show oscillating behavior, which has been noted before for isomers of transition-metal complexes.[25] However, the binding energies of the osmium compounds with NH_3 calculated at MP2 and MP3 are in most cases very similar and should therefore be reliable. Thus, the energy differences between the complexed species such as **2(NH$_3$)** and **3(NH$_3$)** were calculated using the energy difference between **2** and **3** (calculated at QCISD(T)/II + ZPE) and the difference in the binding energies with NH_3 (calculated at MP3/II + ZPE).

(25) (a) Jonas, V.; Frenking, G.; Gauss, J. *Chem. Phys. Lett.* **1992**, *194*, 109. (b) Neuhaus, A.; Frenking, G.; Huber, C.; Gauss, J. *Inorg. Chem.* **1992**, *31*, 5355. (c) Marsden, C. J.; Wolynec, P. P. *Inorg. Chem.* **1991**, *30*, 1681.

(26) Zalkin, A.; Templeton, D. H. *Acta Crystallogr.* **1953**, *6*, 106.

(27) Griffith, W. P.; Skapsi, A. C.; Woode, K. A.; Wright, M. J. *Inorg. Chim. Acta* **1978**, *31*, L413.

(28) When comparing the theoretical and experimental geometries, one should be aware that the bond lengths for osmium bonds taken from X-ray analysis are subject to errors, which are due to the large differences between the atomic numbers of Os and the first-row atoms. This error for the bond length may well be 0.1 Å.

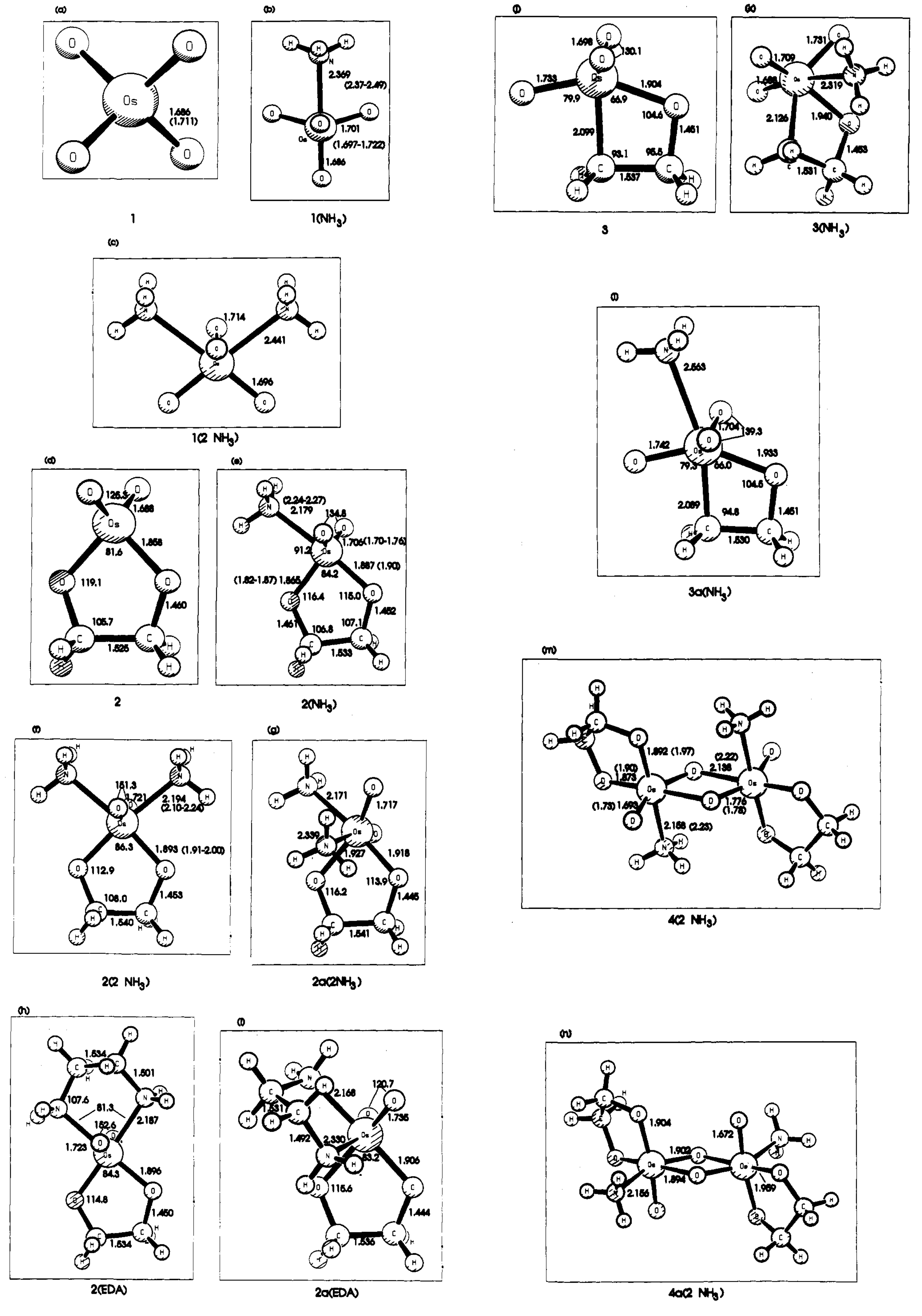

1

1(NH$_3$)

1(2 NH$_3$)

2

2(NH$_3$)

2(2 NH$_3$)

2a(2NH$_3$)

2(EDA)

2a(EDA)

3

3(NH$_3$)

3a(NH$_3$)

4(2 NH$_3$)

4a(2 NH$_3$)

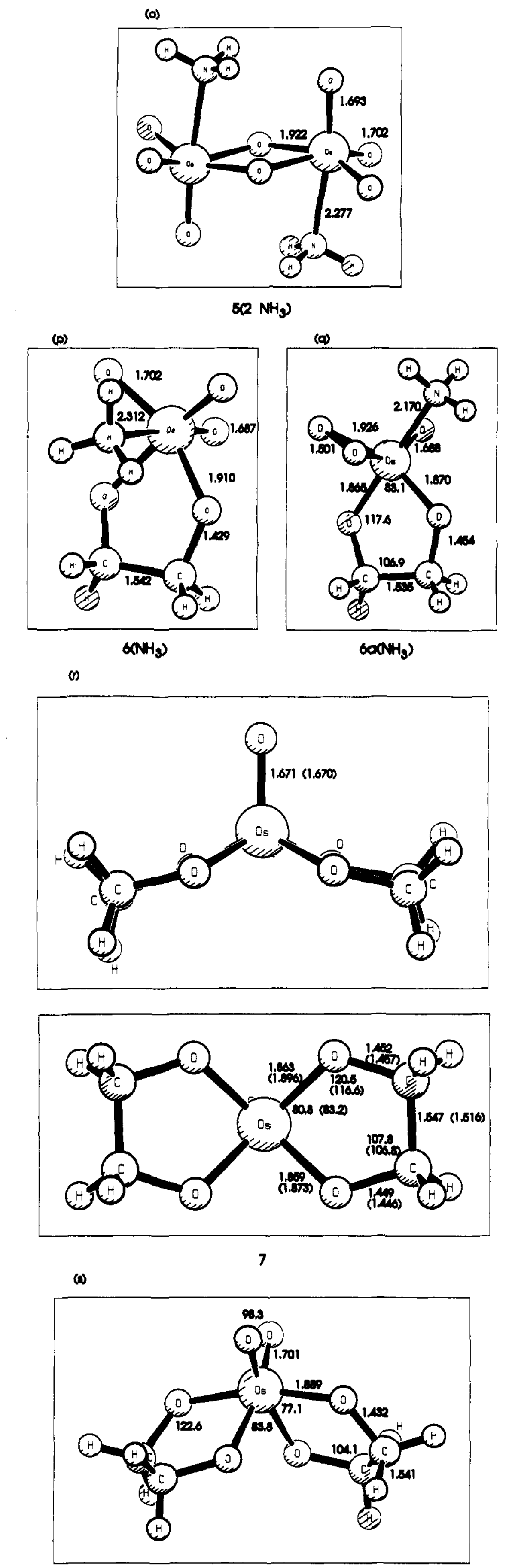

Figure 1. Optimized geometries at HF/I (bond lengths in Å, angles in deg). Experimental values[5e,o,9,12,26,27,32,37] given in parentheses.

orbital (HOMO) relative to **1** (Table 3). The contour line diagrams for the most important orbitals of **1** and **1(NH_3)** are shown in Figure 2. The HOMO of OsO_4 (**1**) is a set of triply degenerate 2p orbitals at oxygen with t_1 symmetry with the eigenvalue $\epsilon_{HOMO} = -14.50$ eV. This orbital has the proper symmetry for interaction with the π^* LUMO of an olefin.[29] The HOMO of **1(NH_3)** is mainly located in the Os–N bonding region, with $\epsilon_{HOMO} = -12.73$ eV. This orbital does not have the right symmetry for interaction with the π^* LUMO of an olefin and is probably not important for the discussion. Slightly lower in energy than the HOMO is a doubly degenerate set of 2p orbitals at oxygen which may interact with the π^* LUMO of the alkene with $\epsilon_{HOMO} = -13.23$ eV. The HOMO-1 of **1(NH_3)** corresponds to the HOMO of **1**. This means that the addition of NH_3 to OsO_4 raises the energy of the HOMO of **1** by 1.17 eV! Also, the LUMO of OsO_4 is *raised* in energy upon complexation by NH_3. The calculated eigenvalue of **1(NH_3)** ($\epsilon_{LUMO} = -0.76$ eV) is higher than that of the LUMO of **1** ($\epsilon_{LUMO} = -1.16$ eV). Because of the orbital energies of the frontier orbitals of **1** and **1(NH_3)**, the oxidation of olefins in the presence of bases might be considered to be nucleophilic attack of **1(NH_3)** on the olefin. This would offer an explanation for the increase in the rate of the addition reaction of OsO_4 to olefins in the presence of bases.[4] However, it has been shown that electron-withdrawing groups on the olefin *retard* its reactivity toward OsO_4.[30] Because electron-withdrawing groups lower the energy level of the LUMO,[31] the experimentally observed[30] decrease in the reaction rate is evidence against a rate-determining nucleophilic reaction step. It will be shown below that an alternative explanation is possible which is based upon the greater stabilization of the reaction product by the ammine.

Does osmium tetraoxide form a stable complex with two molecules of the base **1(2NH_3)**, which then adds to the alkene, or does the complexation by the second base take place *after* **1(NH_3)** has added to the alkene (pathway 2 in Scheme 4)? Burton[13] observed only 1:1 complex formation between OsO_4 and NH_3 but second-order kinetic dependence on ammonia concentration over the same range. Clark and Behrman[14] carried out kinetic measurements of the OsO_4/pyridine system. They came to the conclusion that there is no evidence for a competing process that is first-order in pyridine.[14] However, with the data at hand, they could not adequately distinguish between the different pathways which lead to the pyridine-catalyzed OsO_4–alkene addition product. It should be noted that **1(2NH_3)** is formally a 20-electron complex (if the oxygens are considered as 4-electron donors, O^{2-}) which should not be very stable.

Figure 1 shows the optimized structure of $OsO_4{\cdot}2NH_3$ (**1-(2NH_3)**). The ammonia ligands in **1(2NH_3)** are cis to each other. An isomer with the NH_3 groups in the trans position is not a minimum on the potential energy hypersurface. The Os–N bond length calculated for **1(2NH_3)** is much longer (2.441 Å) than that for **1(NH_3)** (2.369 Å). Also, the calculated complexation energy for the second NH_3 is significantly lower than that for **1(NH_3)**, only 4.0 kcal mol^{-1} at MP2/II + ZPE and even lower (1.7 kcal mol^{-1}) at MP3/II + ZPE (Table 2). But the highest occupied MO of **1(2NH_3)** which can interact with the π^* LUMO of the olefin is raised by another 1.13 eV relative to **1(NH_3)**. The HOMO-2 of **1(2NH_3)** (Figure 2) is composed of the 2p orbitals at the oxygen atoms trans to the NH_3 ligands. The HOMO and HOMO-1 are located mainly in the Os–N bonding region. The eigenvalue $\epsilon_{HOMO\text{-}2}$ of **1(2NH_3)** is −12.10 eV, which is 2.40 eV

---

[29] For a detailed discussion of the orbital interactions between OsO_4 and the base adducts with olefins, see ref 11.

[30] (a) Badger, G. M. *J. Chem. Soc.* **1949**, 456. (b) Henbest, H. B.; Jackson, W. R.; Robb, B. C. G. *J. Chem. Soc. B* **1966**, 803. (c) Sharpless, K. B.; Williams, D. R. *Tetrahedron Lett.* **1975**, 3045. (d) Markó, I. E. *Proceedings of the Chiral Synthesis Symposium and Workshop*; Spring Innovations Ltd.: Stockport, England, 1989; pp 13–21.

[31] Fleming, I. *Frontier Orbitals and Organic Chemical Reactions*; Wiley: New York, 1976.

Table 1. Calculated Total Energies E_{tot} (hartrees), Relative Energies (kcal mol^{-1}), and Zero-Point Vibrational Energies (ZPE, kcal mol^{-1}) for Geometries Optimized at HF/I

		HF/I		HF/II	MP2/II	MP3/II	QCISD(T)/II	
	symmetry	E_{tot}	ZPE (× 0.9)	E_{tot}	E_{tot}	E_{tot}	E_{tot}	E_{rel}
1	T_d	−387.770 21	8.2	−389.554 36	−390.946 38	−390.675 89	−390.861 81	
1(NH$_3$)	C_{3v}	−443.681.67	32.0	−445.745 21	−447.318 57	−447.055 66		
1(2NH$_3$)	C_{2v}	−499.574 71	55.4	−501.924 85	−503.679 68	−503.425 06		
2	C_2	−465.544 14	43.8	−467.698 71	−469.197 88	−469.062 76	−469.206 41	0.0
2(NH$_3$)	C_1	−521.474 44	68.0	−523.909 35	−525.584 49	−525.460 57		0.0
2(2NH$_3$)	C_2	−577.389 56	92.3	−580.113 29	−581.972 38	−581.857 34		0.0
2a(2NH$_3$)	C_1	−577.347 16	91.5	−580.070 15	−581.932 58	−581.814 62		26.0^a
2(EDA)	C_2	−653.850 55	115.4	−657.004 81	−659.118 21			0.0
2a(EDA)	C_1	−653.811 42	114.6	−656.963 28	−659.082 22			21.8^d
3	C_s	−465.399 85	44.0	−467.561 33	−469.188 68	−468.967 16	−469.158 09	30.5^b
3(NH$_3$)	C_1	−521.296 86	66.6	−523.755 22	−525.579 50	−525.356 28		34.3^c
3a(NH$_3$)	C_s	−521.294 04	65.3	−523.745 53	−525.553 09	−525.340 09		43.2^c
4(2NH$_3$)	C_i	−1043.021 03		−1047.845 63	−1051.226 49			
4a(2NH$_3$)	C_i	−1042.966 98		−1047.797 71	−1051.154 95			44.9^f
5(2NH$_3$)	C_{2h}	−87.383 78	66.2	−891.450 37	−894.641 23			
6(NH$_3$)	C_1	−595.749 92	70.1	−598.626 30	−600.643 75	−600.396 22		0.0
6a(NH$_3$)	C_1	−595.831 87	70.1	−598.651 12	−600.510 20	−600.397 53		−0.8^e
7	C_2	−617.668 09	81.9	−620.634 75	−622.550 82			
8	C_2	−691.904 49	82.9	−695.304 38	−697.572 70			
NH$_3$	C_{3v}	−55.872 20	20.3	−56.181 87	−56.349 81	−56.361 78	−56.367 27	
C_2H_4	D_{2h}	−77.600 99	31.1	−78.031 36	−78.281 25	−78.302 87	−78.317 92	

[a] Relative to **2(2NH$_3$)** at MP3/II//HF/I + ZPE. [b] Relative to **2** at QCISD(T)/II//HF/I + ZPE. [c] Relative to **2(NH$_3$)**, using the energy difference **2** – **3** (QCISD(T)/II/HF/I + ZPE) and the stabilization energies by ammonia (reactions 8 and 10, Table 2, MP3/II/HF/I + ZPE). [d] Relative to **2(EDA)** at MP2/II/HF/I + ZPE. [e] Relative to **6** at MP3/II/HF/I + ZPE. [f] Relative to **4(2NH$_3$)** at MP2/II/HF/I.

Table 2. Calculated Reaction Energies (kcal mol^{-1}) for Geometries Optimized at HF/1 (Values in Parentheses Include the ZPE Correction)

no.	reaction	HF/II	MP2/II	MP3/II	QCISD(T)/II
1	**1** + NH$_3$ → **1(NH$_3$)**	−5.6 (−2.1)	−13.9 (−10.5)	−11.3 (−7.8)	
2	**1(NH$_3$)** + NH$_3$ → **1(2NH$_3$)**	+1.4 (+4.5)	−7.0 (−4.0)	−4.8 (−1.7)	
3	**1** + C$_2$H$_4$ → **2**	−70.9 (−66.4)	+18.7 (+23.2)	−52.7 (−48.2)	−16.7 (−12.2)
4	**1** + C$_2$H$_4$ → **3**	+15.3 (+20.0)	+24.5 (+29.2)	+7.3 (+12.0)	+13.6 (+18.3)
5	**1(NH$_3$)** + C$_2$H$_4$ → **2(NH$_3$)**	−83.3 (−78.4)	+9.6 (+14.5)	−64.0 (−59.1)	−28.0 (−23.1)^a
6	**1(NH$_3$)** + C$_2$H$_4$ → **3(NH$_3$)**	+13.4 (+16.3)	+12.8 (+15.7)	+1.4 (+4.3)	+7.7 (+11.2)^a
7	**1(NH$_3$)** + C$_2$H$_4$ → **3a(NH$_2$)**	+19.5 (+21.5)	+29.4 (+31.5)	+11.6 (+13.8)	+17.9 (+20.1)^a
8	**1(2NH$_3$)** + C$_2$H$_4$ → **2(2NH$_3$)**	−96.6 (−90.7)	−7.4 (−1.5)	−81.2 (−75.5)	−45.2 (−39.4)^a
9	**1(2NH$_3$)** + C$_2$H$_4$ → **2a(2NH$_3$)**	−71.5 (−65.5)	+17.8 (+22.8)	−54.4 (−49.4)	−18.4 (−13.4)
10	**2** + NH$_3$ → **2(NH$_3$)**	−18.1 (−14.2)	−23.1 (−19.2)	−22.6 (−18.7)	
11	**2(NH$_3$)** + NH$_3$ → **2(2NH$_3$)**	−13.8 (−9.8)	−23.9 (−19.9)	−22.0 (−18.0)	
12	**2(NH$_3$)** + NH$_3$ → **2a(2NH$_3$)**	+12.3 (+15.5)	+1.1 (+4.3)	+4.8 (+8.0)	
13	**3** + NH$_3$ → **3(NH$_3$)**	−7.5 (−5.2)	−25.7 (−23.4)	−17.2 (14.9)	
14	**3** + NH$_3$ → **3a(NH$_3$)**	−1.5 (−0.5)	−9.2 (−8.2)	−7.0 (−6.0)	
15	2**1(NH$_3$)** → **5(2NH$_3$)**	+25.1 (+24.7)	−2.6 (−3.0)		
16	2**2(NH$_3$)** → **4(2NH$_3$)**	−16.9	−36.1		

[a] Calculated at QCISD(T)/II/HF/I + ZPE using the stabilization energies of NH$_3$ calculated at MP3/II//HF/I + ZPE.[24]

higher than that of **1**. This should make **1(2NH$_3$)** a much more reactive nucleophilic agent than **1(NH$_3$)** and, particularly, **1**. Again, the largest coefficients of the HOMO-2 orbital in **1(2NH$_3$)** are for those atoms trans to the Os–N bond. This means that a nucleophilic attack should preferentially take place via the trans oxygen atoms. The isolated complexes of Os(VI) esters with two molecules of base all show a trans arrangement of the Os–N and Os–O ester bonds.[9,32] It seems conceivable that a complex between OsO$_4$ and *two* molecules of the base present in low concentration adds to the olefinic double bond, rather than **1(NH$_3$)** followed by the addition of the second base. However, recent kinetic studies by Sharpless and co-workers suggest that only a single ligand molecule is involved in the rate-determining step.[5q]

We now discuss the addition products of OsO$_4$ and ethylene. Figure 1 shows the optimized geometries of the five-membered cyclic compound **2** and the four-membered cyclic isomer **3**. Both structures are minima on the potential energy hypersurface. The latter isomer is theoretically predicted to be 30.5 kcal mol^{-1} higher in energy than **2** (QCISD(T)/II + ZPE).[24] The optimized Os–O bond lengths of the four-membered cyclic isomer **3** are significantly longer than those in **2** (Figure 1). The five-membered ring in **2** is calculated to be nonplanar. The smaller bond angles in the four-membered ring of **3** induce a ring strain, which explains why **3** is clearly higher in energy than **2**.

Now we discuss the structures and relative energies of **2** and **3** when they are complexed by ammonia. We calculated two isomers of **2** with one NH$_3$, i.e., **2(NH$_3$)** and **2a(NH$_3$)**, and three isomers of **3** with one NH$_3$, i.e., **3(NH$_3$)**, **3a(NH$_3$)**, and **3b(NH$_3$)**, as shown schematically in Figure 3. The structures **2a(NH$_3$)** and **3b(NH$_3$)** (which has originally been suggested as the chirality-transmitting isomer by Sharpless et al.[5b,c]) are not minima on the potential energy hypersurface. The ammonia ligand dissociates during the geometry optimization. The compounds **2(NH$_3$)**, **3(NH$_3$)**, and **3a(NH$_3$)** are true minima on the potential energy hypersurface (only positive eigenvalues of the Hessian). Structure **3(NH$_3$)** is more stable than **3a(NH$_3$)**, where the energy difference is 15.3 kcal mol^{-1} at MP2/II + ZPE and 8.9 kcal mol^{-1} at MP3/II + ZPE in favor of the former isomer. The Os–N bond is significantly shorter in **3(NH$_3$)** (2.319 Å) than in **3a(NH$_3$)** (2.563 Å, Figure 1). The ammine ligand is far away from the olefin moiety in **3a(NH$_3$)**, but it is in close contact with the olefin in

---

(32) (a) Cartwright, B. A.; Griffith, W. P.; Schröder, M.; Skapski, A. C. *Inorg. Chim. Acta* **1981**, *53*, L129. (b) Kistenmacher, T. J.; Marzilli, L. G.; Rossi, M. *Bioinorg. Chem.* **1976**, *6*, 347. (c) Prangé, T.; Pascard, C. *Acta Crystallogr.* **1977**, *B33*, 621. (d) Neidle, S.; Stuart, D. J. *Biochim. Biophys. Acta* **1976**, *418*, 216. (e) Conn, J. F.; Kim, J. J.; Suddath, F. L.; Blattman, P.; Rich, A. *J. Am. Chem. Soc.* **1976**, *96*, 7152.

Table 3. Energies (eV) and Square of the MO Coefficients, C_i^2, of the High-Lying Occupied Molecular Orbitals

1

MO	ε	C_i^2 O	C_i^2 Os
25 HOMO	-14.50	0.175 47	0.00
24	-14.50	0.175 47	0.00
23	-14.50	0.175 47	0.00
22	-15.71	0.141 27	0.070 32

1(NH$_3$)

MO	ε	C_i^2 O[a]	C_i^2 O[b]	C_i^2 N	C_i^2 Os
29 HOMO	-12.73	0.031 52	0.126 48	0.364 53	0.015 68
28	-13.23	0.309 68	0.186 89	0.004 53	0.002 31
27	-13.23	0.309 68	0.076 51	0.004 53	0.002 31
26	-13.52	0.0	0.230 34	0.00	0.00

1(2NH$_3$)

MO	ε	C_i^2 O[a]	C_i^2 O[b]	C_i^2 N	C_i^2 Os
34 HOMO	-11.73	0.040 86	0.184 77	0.156 28	0.024 80
33	-11.78	0.049 75	0.160 40	0.181 39	0.013 97
32	-12.10	0.268 04	0.084 66	0.003 35	0.001 25
31	-12.38	0.198 00	0.146 04	0.002 26	0.002 15

[a] Oxygen trans to nitrogen. [b] Oxygen cis to nitrogen.

3(NH$_3$) (Figure 1). Because the energy calculations indicate that **3(NH$_3$)** is clearly the more stable four-membered cyclic isomer, we will compare only **3(NH$_3$)** with the five-membered cyclic structure **2(NH$_3$)**.

Figure 1 shows that the geometries of the cyclic moieties in **2(NH$_3$)** and **3(NH$_3$)** are not very different from those of **2** and **3**, respectively. The Os–N bond is clearly shorter in **2(NH$_3$)** (2.179 Å) than in **1(NH$_3$)** (2.369 Å). Although the Os–N bond length in **3(NH$_3$)** is longer (2.319 Å) than that in **2(NH$_3$)** (2.179 Å), the stabilization of the four-membered cyclic intermediate by ammonia is comparable (23.4 kcal mol^{-1} at MP2/II + ZPE, 14.9 kcal mol^{-1} at MP3/II + ZPE) to that of the five-membered cyclic isomer (19.2 kcal mol^{-1} at MP2/II + ZPE, 18.7 kcal mol^{-1} at MP3/II + ZPE, Table 2). The stabilization of **2** and **3** by ammonia is significantly higher, however, than the stabilization of OsO_4 (10.5 kcal mol^{-1} at MP2/II + ZPE, 7.8 kcal mol^{-1} at MP3/II + ZPE). This is important for the discussion of the reaction mechanism below.

The calculated geometry of **2(NH$_3$)** may be compared with the experimental geometry of the related cinchona–alkaloid complexes of Os(VI) esters determined by X-ray analysis.[5o] The observed Os–N distances are 2.243(5) and 2.27(2) Å, shorter than the experimental Os–N distances in the corresponding OsO_4–alkaloid complex (2.49 Å).[5e,28] The shortening of the Os–N bond upon formation of the Os(VI) ester is in agreement with the calculated Os–N interatomic distances of **1(NH$_3$)** and **2(NH$_3$)**. Also, the other calculated geometrical variables of **2(NH$_3$)** compare very well with the experimental values, as shown in Figure 1.

We investigated the complexes of **2** and **3** with two molecules of ammonia. Figure 1 shows the optimized structure of **2(2NH$_3$)**. A complex of **3** with two molecules of ammonia, i.e., **3(2NH$_3$)**, is not a minimum on the potential energy hypersurface. An attempt to optimize the geometry of **3(2NH$_3$)** yields **3(NH$_3$)** and NH_3.

The Os–N bond lengths in **2(2NH$_3$)** are only slightly longer (2.194 Å) than those in **2(NH$_3$)** (2.179 Å). The calculated complexation energy of the second ammonia is comparable in magnitude (18.0 kcal mol^{-1}, MP3/II + ZPE) to the first complexation energy (18.7 kcal mol^{-1}, MP3/II + ZPE, Table 2). The ring geometries of **2(2NH$_3$)** and **2(NH$_3$)** are very similar (Figure 1). The optimized geometry of **2(2NH$_3$)** compares favorably with experimentally reported geometries of pyridine-complexed Os(VI) esters obtained by X-ray analysis.[9,32] The markedly nonlinear O=Os=O angle calculated as 151.3° and the direction of bending, away from the five-membered ring toward the nitrogen atoms, are in good agreement with the experimental observations[32] (O=Os=O ~164°). The experimental Os=O bond length in these complexes is ~1.72 Å, which is exactly what is calculated here.[9,32] The experimentally observed[9,32] Os–N bond lengths in the pyridine complexes are 2.10–2.24 Å, which is in the range of the Os–N distance calculated for **2(2NH$_3$)** (2.19 Å). The reported Os–O bond lengths are slightly longer (1.91–2.00 Å)[9,32] than those calculated for **2(2NH$_3$)** (1.893 Å).

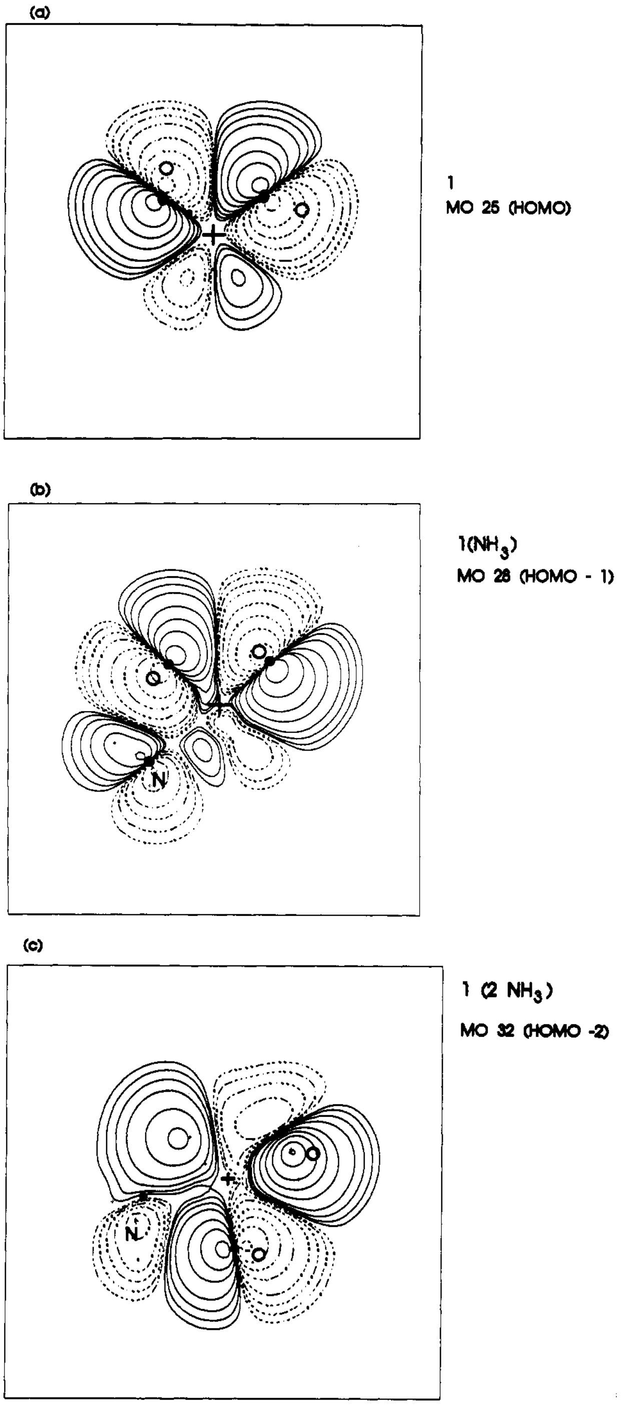

Figure 2. Contour line diagrams of the high-lying occupied MOs with proper symmetry for **1**, **1(NH$_3$)**, and **1(2NH$_3$)** in the O–Os–O plane (**1**) and N–Os–O_{trans} plane (**1(NH$_3$)**, **1(2NH$_3$)**). The position of the Os atom is indicated by a cross (+), and the positions of the other atoms in the plane are shown by solid circles.

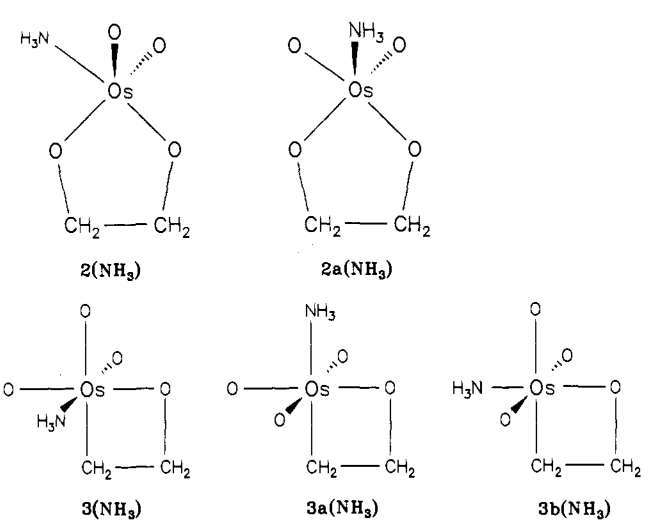

Figure 3. Schematic representation of the isomeric structures **2(NH$_3$)**, **2a(NH$_3$)**, **3(NH$_3$)**, **3a(NH$_3$)**, and **3b(NH$_3$)**.

Scheme 4. Schematic Representation of the Two Pathways 1 and 2 for the Consecutive Addition of the Second Ligand L and the Olefin to **1(L)**

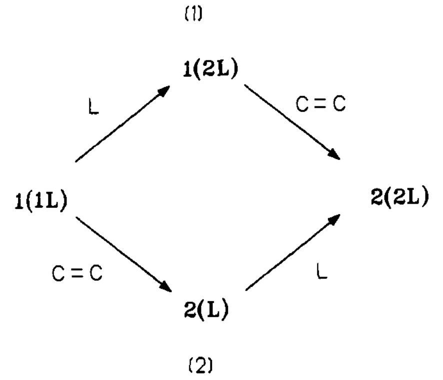

We optimized an isomeric structure of **2(2NH$_3$)** with one NH$_3$ in an axial position as a minimum on the potential energy surface, i.e., molecule **2a(NH$_3$)** (Figure 1). Structure **2a(2NH$_3$)** is clearly less stable than **2(2NH$_3$)**. At the MP3/II + ZPE level of theory, **2a(2NH$_3$)** is predicted to be 26.0 kcal mol^{-1} higher in energy than **2(2NH$_3$)** (Table 1).

Figure 4 shows the relative energies of the calculated structures. The addition of OsO$_4$ (**1**) to ethylene, yielding **2**, is theoretically predicted to be *exothermic* by 12.2 kcal mol^{-1} (Table 2). In contrast, the formation of **3** is 18.3 kcal mol^{-1} *endothermic*. The formation of the four-membered and five-membered cyclic structures becomes energetically more favored in the presence of one molecule of ammonia. The addition of ethylene to **1(NH$_3$)**, yielding **2(NH$_3$)**, is 23.1 kcal mol^{-1} exothermic, and the [2 + 2] addition yielding **3(NH$_3$)** is 11.2 kcal mol^{-1} endothermic (MP3/II + ZPE, Table 2). Thus, the [2 + 2] and [3 + 2] cycloaddition reactions of the olefin and OsO$_4$ are predicted to become thermodynamically more favorable in the presence of a base. Although we could not optimize the transition states for the formation of **2(NH$_3$)** and **3(NH$_3$)**,[33] the Hammond postulate[34] suggests that the activation barriers for the addition reactions in the presence of ammonia should be lower than those for the formation of **2** and **3**, respectively. This might explain the acceleration of the addition reaction in the presence of bases.[4] Although the formation of **3(NH$_3$)** is calculated to be endothermic, the rather low reaction energy of 11.2 kcal mol^{-1} suggests that the [2 + 2] cycloaddition product is initially formed as a short-lived intermediate. The value of 11.2 kcal mol^{-1} may even be too high. If the binding energies of NH$_3$ calculated at MP2/II are used, the formation of **3(NH$_3$)** from **1(NH$_3$)** and ethylene is only 5.3 kcal mol^{-1} endothermic.[35] The enantioselectivity might then be due to the close proximity of the ammine to the olefin moiety in **3(NH$_3$)**. The steric interactions should have an influence upon both reaction steps, the [2 + 2] addition yielding **3(NH$_3$)** and the rearrangement toward **2(NH$_3$)**. This would explain the experimentally observed kinetic temperature effects of the asymmetric dihydroxylation.[5p]

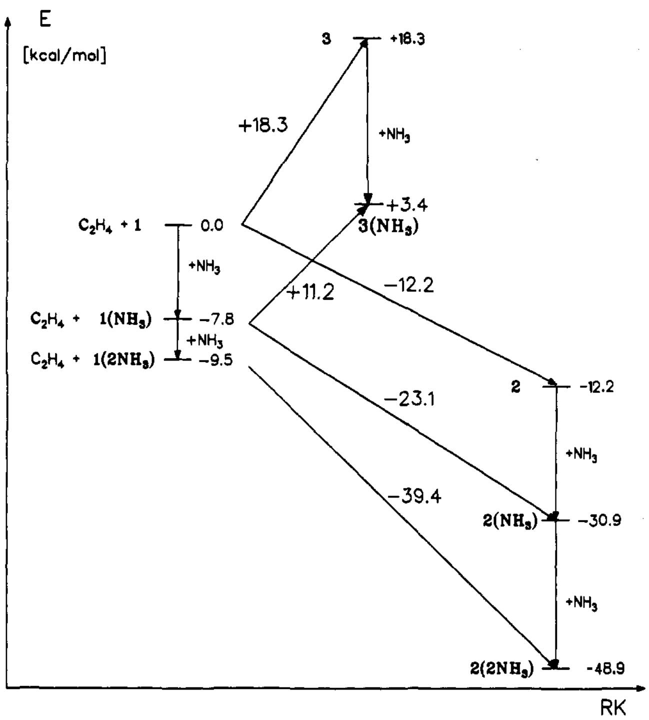

Figure 4. Calculated reaction profile for the osmylation reaction. The energies are taken from Table 2.

Now we turn to the reaction mechanism proposed by Corey[7] (Scheme 2). Structure **2a(2L)** has been suggested as the messenger intermediate for the chiral information if bidentate ligands are used.[7a] The ammonia ligand trans to the Os=O bond is in close proximity of the olefin and could, in principle, be responsible for the transfer of the chiral information. As shown above, the isomeric structure **2a(2NH$_3$)** is calculated to be 24.2 kcal mol^{-1} higher in energy than **2(2NH$_3$)** (MP2/II + ZPE, Table 1). The calculated stability difference does not change significantly when a bidentate ligand rather than two molecules of ammonia is employed. Figure 1 shows the optimized structures of the two isomers with ethylenediamine (EDA) instead of 2NH$_3$. Structure **2(EDA)** is calculated to be 21.8 kcal mol^{-1} lower in energy than **2a(EDA)**. The energy difference between the two isomeric forms is rather insensitive to the level of theory. At HF/II + ZPE, **2a(EDA)** is 25.2 kcal mol^{-1} higher in energy than **2(EDA)**.

Two different [3 + 2] cycloaddition reactions have to be considered for the Corey mechanism[7] for bidentate ligands. The formation of **2(2NH$_3$)** from **1(2NH$_3$)** and ethylene is calculated to be 39.4 kcal mol^{-1} exothermic (Table 2, reaction 8). Also, the formation of the higher lying isomer **2a(2NH$_3$)** from **1(2NH$_3$)** and ethylene is still exothermic by 13.4 kcal mol^{-1} (Table 2, reaction 9). However, structure **2a(2NH$_3$)** is not stable toward loss of the axial ammonia group. The formation of **2a(2NH$_3$)**

---

(33) Preliminary calculations indicate that the optimization of the transition state has to be carried out at a correlated level of theory.

(34) Hammond, G. S. *J. Am. Chem. Soc.* **1955**, *77*, 334.

(35) The formation of the four- and five-membered cyclic structures is also influenced by the entropy of the reaction and the solvent effects. The free energy of the cyclic structures is probably higher than the enthalpy, because the complexation reaction can be expected to have a large negative ΔS. However, the cyclic complexes are probably more stabilized by polar solvents than the starting materials, which might partly compensate for the entropy contributions.

from **2(NH$_3$)** and NH_3 is 8.0 kcal mol^{-1} endothermic (Table 2, reaction 12). There are other arguments against the formation of **2a(2NH$_3$)**. The oxygen atoms trans to the nitrogen are more nucleophilic than the cis oxygens, as revealed by the coefficients of the HOMO-2 of **1(NH$_3$)** and **1(2NH$_3$)** (see discussion above). A nucleophilic attack should therefore for electronic reasons be directed toward **2(2L)** but not toward **2a(2L)**. There are several structures known which correspond to **2(2L)**[9,32] but not for **2a(2L)**. Still, this does not rule out the formation of **2a(2L)** as an intermediate if steric biases favor the formation of **2a(2L)** over **2(2L)**.

A different mechanism involving the formation of the dimeric species **4(2L)** (Scheme 2) was suggested by Corey[7b] for the enantioselective addition of OsO_4 to olefins in the presence of monodentate ligands such as the cinchona alkaloids.[5] We optimized the geometry of **4(2NH$_3$)** as shown in Figure 1. The theoretically predicted geometry is in good agreement with the X-ray structure of the related dimeric osmium tetraoxide adduct with quinuclidine and cyclohexene.[12] The calculations predict an asymmetric bridge with two long (2.136 Å) and two short (1.776 Å) Os–O bonds. The experimentally observed structure[12] shows Os–O bond lengths of 1.78 and 2.22 Å for the Os_2O_2 bridge (Figure 1). The good agreement of the completely geometry-optimized structure **4(2NH$_3$)** with the experimental values shown in Figure 1 is particularly gratifying considering the size of the molecule. It demonstrates the power of ECP methods for predicting the geometries of transition-metal complexes. The calculated Os–N bond length in **4(2NH$_3$)** is slightly shorter (2.158 Å) than that in **2(NH$_3$)** (2.179 Å), which indicates higher complex stabilization. The formation of **4(2NH$_3$)** from two molecules **2(NH$_3$)** is calculated at MP2/II to be 36.1 kcal mol^{-1} exothermic (Table 2). At HF/II, the reaction is thermodynamically favored by 16.9 kcal mol^{-1}. The dimeric quinuclidine complex of OsO_4 with cyclohexene **4(2L)** is monomeric in chloroform.[12] This may be caused by the interactions of the monomer **2(L)** with the solvent or may just be an entropy effect.

Corey[7b] postulated that **4(2L)** is formed by addition of dimeric **1(L)** to the olefin. Figure 1 shows the optimized geometry of **5(2NH$_3$)**, the dimer of **1(NH$_3$)**. There are no experimental data available for comparison with **5(2NH$_3$)**, which is predicted by the calculations to be a minimum on the potential energy hypersurface. Unlike in **4(2L)**, the Os_2O_2 unit in **5(2L)** has a *symmetric* bridge with four identical Os–O bond lengths. Structure **5(2NH$_3$)** has C_{2h} symmetry and Os–N bond lengths which are clearly shorter (2.277 Å) than those in monomeric **1(NH$_3$)** (2.369 Å). The formation of **5(2NH$_3$)** from two molecules of **1(NH$_3$)** is calculated to be nearly thermoneutral at MP2/II + ZPE (−3.0 kcal mol^{-1}, reaction 13, Table 2) but endothermic at HF/II + ZPE (+25.1 kcal mol^{-1}). Because of the rather large difference between the MP2 and HF results, the absolute numbers may not be very accurate. The calculations indicate, however, that the formation of the dimeric structure **4(2NH$_3$)** from **2(NH$_3$)** is energetically more likely than the dimerization of **1(2NH$_3$)**, yielding **5(2NH$_3$)** (Table 2, reactions 15 and 16).

A recent examination of the steric requirements for the formation of a dimeric adduct in the presence of dihydroquinone ethers led Corey to suggest[7c] that a different isomer of **4(2L)**, i.e., structure **4a(2L)**, which has the ligands L in an equatorial position, might be the actual intermediate. Complex **4a(2L)** would then be formed by addition of the olefin to an isomer of **5(2L)** with equatorial NH_3 groups. We optimized the geometry of **4a(2NH$_3$)** (Figure 1). The calculated energies predict that **4a(2NH$_3$)** is much higher in energy than **4(2NH$_3$)**. The latter isomer is 28.6 kcal mol^{-1} more stable than **4a(2NH$_3$)** at HF/II. At MP2/II, the energy difference in favor of **4(2NH$_3$)** is even higher (41.6 kcal mol^{-1}). The isomeric structure **5a(2NH$_3$)**, with equatorial ammonia ligands, is not a minimum on the potential energy surface. Thus, the formation of **4a(2NH$_3$)** in the addition reaction of OsO_4 to ethylene in the presence of ammonia is highly unlikely.

We calculated the structures **6(NH$_3$)**, **7**, and **8**, which have been suggested by Sharpless[5f] as intermediates for the second reaction cycle showing low enantioselectivity (Scheme 3). Figure 1 shows the optimized geometry of the central intermediate **6(NH$_3$)**. The Os–N bond length is clearly longer than that in **2(NH$_3$)** but shorter than that in **1(NH$_3$)**. The Os–O bond lengths of the cyclic moiety are longer in **6(NH$_3$)** than in **2(NH$_3$)**, but otherwise the structure looks reasonable. We also optimized the geometry of the isomeric form **6a(NH$_3$)**, which has the ammonia ligand trans to the ring. The calculations predict that **6a(NH$_3$)** does not have three Os=O bonds. Rather, a peroxo complex was calculated as an energy minimum structure, as shown in Figure 1. Peroxo complexes are known for many transition metals, in particular for the early transition elements.[36] Structure **6a(NH$_3$)** is calculated to be 83.8 kcal mol^{-1} higher in energy than **6(NH$_3$)** (MP2/II/HF/I, Table 1). This energy value is not very reliable, however, because **6(NH$_3$)** and **6a(NH$_3$)** have a different coordination around osmium.[24] The two isomers have nearly the same energy at MP3/II//HF/I (Table 1).

Figure 1 shows that the optimized geometry for **7** is in satisfactory agreement with the experimentally derived[17] bond lengths and angles. The optimized geometry of **8** appears reasonable and shows no surprising features. There are no experimental data available for complexes **6(NH$_3$)** and **8** or derivatives thereof. The calculations show that the intermediates of the catalytic two-cyclic-reaction course suggested by Sharpless[5f] are indeed minima on the potential energy hypersurface.

4. Summary

The theoretical results presented in this study allow the following conclusions with regard to the postulated reaction mechanisms[2-10] for the addition of OsO_4 to olefins in the presence of a base. The two-step mechanism with initial [2 + 2] cycloaddition, yielding the four-membered cyclic intermediate **3(L)**, followed by rearrangement and formation of the five-membered cyclic species **2(L)** and eventually **2(2L)** suggested by Sharpless et al.[5b,c] (Scheme 1) is possible. The structure **3(NH$_3$)** is a genuine minimum on the potential energy hypersurface. Although **3(NH$_3$)** is calculated to be 32.3 kcal mol^{-1} higher in energy than the isomeric form **2(NH$_3$)**, the formation of **3(NH$_3$)** from **1(NH$_3$)** and ethylene is only 11.2 kcal mol^{-1} endothermic. This may well be below the activation barrier for the addition reaction. Because the ammine moiety in **3(NH$_3$)** is in close proximity to the olefin, the formation of **3(L)** in a rate-determining step is a possible explanation for the enantioselectivity, which is observed in addition of OsO_4 to olefins in the presence of a chiral base. This would also offer a rationalization for the stereoelectronic control which is found in the reaction.[8,9]

The calculations show also that the HOMO of OsO_4 is significantly raised in energy upon complexation by ammonia. This could mean that the addition reaction should be considered to be a nucleophilic attack of **1** on the olefin. However, the greater stabilization of the cyclic addition products **2** and **3** by NH_3 over the starting material **1**, which makes the addition reaction thermodynamically more favored, indicates that the activation barrier of the base-catalyzed reaction should be lower than that of the reaction without the base. In the light of the present results, it seems possible that the initial reaction is a [2 + 2] cycloaddition with a nucleophilic phase, in which one oxygen atom attacks an olefinic carbon, and an electrophilic phase, in which the other olefinic carbon attacks the osmium atom, yielding **3(L)**. This would also be a plausible explanation for the stereoelectronic

---

(36) (a) Connor, J. A.; Ebsworth, E. A. V. *Adv. Inorg. Chem. Radiochem.* **1964**, *6*, 279. (b) Mimoun, H. In The Chemistry of Peroxides; Patai, S., Ed.; Interscience: New York, 1983; p 463.

(37) Phillips, F. L.; Skapski, A. C. *Acta Crystallogr.* **1975**, *B31*, 1814.

effects, which are observed in the addition reaction.[8] The recently reported addition of OsO_4 to fluoroolefins in the presence of pyridine, in which the polar difluorovinylidene F_2CCH_2 was found to be the most reactive olefin, could be explained in the same fashion.[9] Although the present calculations do not prove the mechanism, they provide the first theoretical evidence based upon ab initio results that the mechanism shown in Scheme 1 is possible.

The formation of the isomeric five-membered cyclic species **2a(2L)** rather **2(2L)** in a [3 + 2] cycloaddition, as suggested for bidentate ligands by Corey,[7a] is also energetically possible if steric biases favor the former isomer. The calculations show that **2(2NH$_3$)** and **2a(2NH$_3$)** are minima on the potential energy hypersurface. The addition reaction of **1(2NH$_3$)** and ethylene leading to **2(2NH$_3$)** is 39.4 kcal mol^{-1} exothermic, and the formation of **2a(2NH$_3$)** is still 13.4 kcal mol^{-1} exothermic. However, structure **2a(2NH$_3$)** is unstable toward loss of one NH_3. Also, the shape of the HOMO of **1(2NH$_3$)** suggests that the addition of ethylene should be directed toward **2(2NH$_3$)** rather than toward **2a(2NH$_3$)**. The postulated[7b,c] formation of the dimer **4(2NH$_3$)** from **5(2NH$_3$)** and ethylene is possible. The recently proposed[7c] isomeric dimer **4a(2NH$_3$)**, however, is calculated to be much higher in energy than **4(2NH$_3$)**. The formation of **4a(2NH$_3$)** appears highly unlikely, also because the postulated educt dimer **5a(2NH$_3$)** is not a minimum on the potential energy hypersurface.

The theoretical results cannot rule out the reaction mechanism suggested by Corey (Scheme 2). At present, the mechanism suggested by Sharpless appears to be more plausible to us, because an initial [2 + 2] cycloaddition with a nucleophilic and then an electrophilic phase would explain the electronic effects[8,9] without invoking steric biases. Such a mechanism is also in accord with the results of the kinetic measurements by Sharpless et al.,[5p] which unequivocally show an inversion point in the Eyring diagram of the dihydroxylation. Also, the formation of the isomeric dimer **4a(2L)**, which was recently proposed by Corey,[7c] is shown by our calculations to be highly unlikely.

Finally, we want to point out that the theoretically predicted geometries using ECP methods and moderate valence basis sets for the osmium compounds reported in this work are generally in good agreement with experimental values. The results presented here and in other work[1,17-19] demonstrate that ab initio methods can be very helpful not only for the chemistry of the first and second full rows of the periodic systems[38] but also for compounds of heavy elements such as the transition metals.

Addendum

During review, a theoretical study using density functional theory appeared about the addition of ethylene to RuO_4.[39] The results are similar to our work.

Acknowledgment. Stimulating discussions with Dr. J. J. Wolff are gratefully acknowledged. We thank the Hochschulrechenzentrum of the Philipps-Universität Marburg, the Hessischer Höchstleistungsrechner (HHLR) Darmstadt, and HLRZ Jülich for their excellent service. Additional support was given by the computer companies Silicon Graphics and Convex. This study has been supported financially by the Deutsche Forschungsgemeinschaft (SFB 260) and the Fonds der Chemischen Industrie. We thank Prof. K. B. Sharpless and Dr. P.-O. Norrby for sending us their results and preprints prior to publication.

---

(38) Hehre, W. J.; Radom, L.; Schleyer, P. v. R.; Pople, J. A. *Ab Initio Molecular Orbital Theory*; Wiley: New York, 1986.

(39) Norrby, P.-O.; Kolb, H. C.; Sharpless, K. B. *Organometallics* **1994**, *13*, 344.